Spin splitting in symmetrical SiGe quantum wells

L. E. Golub* and E. L. Ivchenko
A. F. Ioffe Physico-Technical Institute, Russian Academy of Sciences, 194021 St. Petersburg, Russia
(Received 16 October 2003; revised manuscript received 27 January 2004; published 25 March 2004)

Spin splitting of conduction electron states has been analyzed for all possible point symmetries of SiGe quantum well structures. A particular attention is paid to removal of spin degeneracy caused by the rotoinversion asymmetry of a (001) heterointerface between two diamond-lattice materials. The asymmetry is shown to result in spin splitting of both Rashba and Dresselhaus types in symmetrical SiGe quantum wells. Consequences of the spin splitting on spin relaxation are discussed.

DOI: 10.1103/PhysRevB.69.115333 PACS number(s): 71.70.Ej, 72.25.Rb, 75.10.Dg

I. INTRODUCTION

Spin properties attract the great attention in recent years due to attempts to realize an electronic device based on the spin of carriers. Conduction electrons are obvious candidates for such devices, particularly in nanostructures where electron energy spectrum and shape of the envelope functions can be effectively engineered by the growth design, application of electric or magnetic fields as well as by illumination with light.

Various semiconductor materials are being involved in the spintronics activities. SiGe quantum well (QW) structures are among them.[1–4] Although bulk Si and Ge have an inversion center, QW structures grown from these materials can lack such a center and allow the spin splitting of the electronic subbands.

The quantum engineering of spintronic devices is usually focused on the Rashba spin-dependent term to the electron effective Hamiltonian in heterostructures. This contribution appears due to asymmetry of the heteropotential (the so-called structure inversion asymmetry, or SIA) and has no relation to the properties of a bulk semiconductor.

In III-V heterostructures, there exists another spin-dependent contribution called the Dresselhaus term that appears due to bulk inversion asymmetry (BIA). It is commonly believed that the Dresselhaus contribution is absent in structures grown from centrosymmetric materials.

In the present work we show that the Dresselhaus-like spin splitting is possible in heterostructures made of Si and Ge due to the anisotropy of chemical bonds at interfaces.

II. SYMMETRY ARGUMENTS

Symmetry of a (001)-grown interface between $Si_{1-x}Ge_x$ and Si can be C_{2v} or C_{4v} on average.[5] The former point group describes the symmetry of an ideal heterointerface with the interfacial chemical bonds lying in the same plane. A nonideal interface containing monoatomic fluctuations has two kinds of flat areas with interfacial planes shifted with respect to each other by a quarter of the lattice constant. The local symmetry of each area is C_{2v} as well. However if the both kinds are equally distributed, the interface overall symmetry increases up to C_{4v}. It follows then that the symmetry of a $Si_{1-x}Ge_x$/Si QW structure containing two interfaces is described by one of five point groups: D_{2d} or D_{2h} in case of two ideal interfaces with odd or even number of monolayers between them; C_{2v} for a pair of ideal and rough interfaces; C_{4v} or D_{4h} for two nonideal interfaces of the overall symmetry C_{4v} each, see Fig. 1.

Two of the above-mentioned groups, D_{4h} and D_{2h}, contain the space inversion operation and forbid the spin splitting of electronic states. Three remaining groups allow the spin-dependent linear-in-$\boldsymbol{k}$ term $\mathcal{H}_{\boldsymbol{k}}=\gamma_{\alpha\beta}\sigma_\alpha k_\beta$. Here σ_α are the Pauli matrices and $\boldsymbol{k}=(k_x,k_y)$ is the in-plane electron wave vector.

In $Si_{1-x}Ge_x$/Si QWs grown along direction $z\|[001]$ with low enough content of Ge in the alloy layer, the lowest conduction band is located near the X point of the Brillouin zone. Note that in the following we consider the electronic states attached to the X_z valley because, due to the quantum confinement effect, its bottom lies lower than X_x and X_y valleys.[6] Hereafter the subscripts x,y,z indicate three X valleys as well as the Cartesian coordinate system with $x\|[100]$, $y\|[010]$ being the in-plane axes. The symmetry analysis of the electron quantum confined states is based on the fact that at the X point the bulk Bloch functions form projective representations of the point group D_{4h}. All five above-mentioned groups are subgroups of D_{4h}. In the group D_{2d}, the Dresselhaus-like term

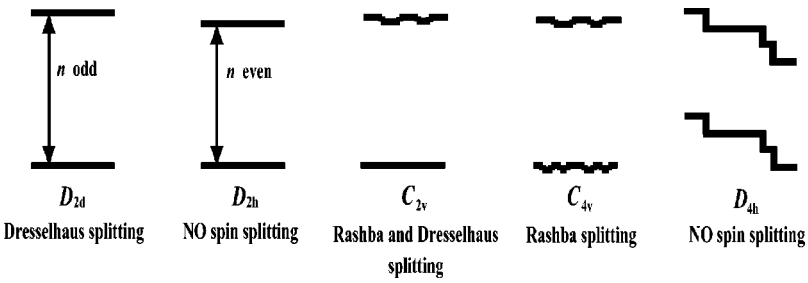

FIG. 1. Different interface profiles and QW point symmetries. The growth direction is [001], n is a number of monoatomic layers.

$$h_D(\boldsymbol{k}) = \sigma_x k_x - \sigma_y k_y$$

is an only invariant which can be constructed from the products $\sigma_\alpha k_\beta$. On the contrary, in the group C_{4v}, the only invariant combination is the Rashba term

$$h_R(\boldsymbol{k}) = \sigma_x k_y - \sigma_y k_x .$$

The analysis shows that both combinations $h_D(\boldsymbol{k})$ and $h_R(\boldsymbol{k})$ are invariants of the group C_{2v}, i.e., both Dresselhaus- and Rashba-like spin-dependent terms are allowed.

In SiGe/Si QWs with high Ge content, the lowest conduction band may be located at the L point. The bulk Bloch functions form projective representations of the D_{3d} point group which are p equivalent to the usual representations of the same group. In this case the associated coordinate system x',y',z' is connected with the valley principal axis $z' \| [111]$ and the in-plane axes $x' \| [1\bar{1}0]$ (perpendicular to one of the mirror-reflection planes) and $y' \| [11\bar{2}]$. In (001)-grown QWs of the symmetry D_{2h} or D_{4h}, intersection of these point groups with D_{3d} is C_{2h} with the inversion, so that the spin degeneracy is retained. On the other hand, the intersection of the rest three groups with D_{3d} is C_s. As a result, the effective Hamiltonian for the L-valley electrons in QWs of the symmetry D_{2d}, C_{2v} or C_{4v} contains three linearly independent combinations $\sigma_{y'}k_{x'}$, $\sigma_{z'}k_{x'}$, and $\sigma_{x'}k_{y'}$ responsible for the spin splitting.

SiGe/Si heterostructures grown in the (111)-direction have either D_{3d} or C_{3v} point symmetry depending on the parity of monolayer numbers. The D_{3d} group has the inversion center and retains the spin degeneracy whereas the C_{3v} group allows the spin splitting. The lowest conduction band in (111)-SiGe/Si QWs is located at the L point of the Brillouin zone. Since C_{3v} is a subgroup of D_{3d}, the relevant symmetry is C_{3v}, and the invariant combination of the products $\sigma_\alpha k_\beta$ is the Rashba term

$$\sigma_{x'}k_{y'} - \sigma_{y'}k_{x'} .$$

III. MICROSCOPIC THEORY

A. Spin splitting of X-valley electrons in (001)-grown QWs

Microscopically, a linear-in-$\boldsymbol{k}$ correction to the conduction-band effective Hamiltonian is given by the second order of the perturbation theory

$$\Delta\mathcal{H} = \frac{H_{SO}H_{\boldsymbol{kp}}^{\dagger} + H_{\boldsymbol{kp}}H_{SO}^{\dagger}}{E_c - E_v}. \tag{1}$$

Here $H_{\boldsymbol{kp}}$ and H_{SO} are interband $\boldsymbol{k}\cdot\boldsymbol{p}$ and spin-orbit interaction Hamiltonians, respectively. We take into consideration only the coupling of the conduction X_1 states and the valence X_4 states. The symmetry properties of the Bloch functions at the X point of a diamond-lattice semiconductor crystal coincide with those of the following functions[7]

$$X_1 \text{ states} \quad \begin{cases} S = \cos(2\pi z/a) \\ Z = \sin(2\pi z/a), \end{cases} \tag{2}$$

TABLE I. Irreducible representations of the C_{2v} group and examples of their basic functions and matrices. The axes x' and y' are parallel to the crystallographic directions $[1\bar{1}0]$, [110].

Representation	Basic functions	Basic matrices
A^+	k_z	
A^-	$k_{x'}k_{y'}$; σ_z	
B^+	$k_{y'}$; $\sigma_{x'}$	$\hat{M}_3$; $\hat{M}_4$
B^-	$k_{x'}$; $\sigma_{y'}$	$\hat{M}_1$; $\hat{M}_2$

$$X_4 \text{ states} \quad \begin{cases} X = \sin(2\pi x/a)\cos(2\pi y/a) \\ Y = \cos(2\pi x/a)\sin(2\pi y/a), \end{cases} \tag{3}$$

where a is the lattice constant. For the bulk states X_1, X_4 in the bases (2), (3), the interband matrix elements can be presented as

$$H_{\boldsymbol{kp}} = \mathcal{P}\begin{pmatrix} k_x & k_y \\ -k_y & -k_x \end{pmatrix}, \quad H_{SO} = \mathcal{U}\begin{pmatrix} \sigma_x & -\sigma_y \\ -\sigma_y & \sigma_x \end{pmatrix}. \tag{4}$$

Here $\mathcal{P} = (\hbar/m_0)\langle S|\hat{p}_x|X\rangle$, $\mathcal{U} = \langle S|U_x|X\rangle$, $\hat{\boldsymbol{p}}$ is the momentum operator, and the pseudovector $\boldsymbol{U} = (\hbar/4m_0^2c^2)\boldsymbol{\nabla}W \times \hat{\boldsymbol{p}}$ enters into the spin-orbit Hamiltonian $H_{SO} = \boldsymbol{\sigma}\cdot\boldsymbol{U}$ (W is the microscopic potential).

The substitution of Eq. (4) into Eq. (1) results in

$$\Delta\mathcal{H} \propto h_D(\boldsymbol{k})\begin{pmatrix} 1 & 0 \\ 0 & -1 \end{pmatrix},$$

where the second multiplier is a 2×2 matrix related to the basis (2). The matrix $\Delta\mathcal{H}$ *does not* lead to lifting the degeneracy of the X_1 states in the bulk centrosymmetric material, in accordance with the general symmetry consideration.

The splitting can be achieved if one takes into account the anisotropy of chemical bonds at the interfaces. It results in δ-functional contributions to the Hamiltonians $H_{\boldsymbol{kp}}$ and H_{SO} of the form

$$\Delta H_{\boldsymbol{kp}} = V_{\boldsymbol{kp}}\delta(z - z_{if}), \quad \Delta H_{SO} = V_{SO}\ \delta(z - z_{if}), \tag{5}$$

where z_{if} is the interface coordinate. The matrices $V_{\boldsymbol{kp}}, V_{SO}$ have few linearly independent components and can be constructed by using the method of invariants. In the latter the 2×2 interband matrices $V_{\boldsymbol{kp}}, V_{SO}$ are decomposed into products $\hat{M}_j k_\alpha$ or $\hat{M}_j\sigma_\alpha$, where $\hat{M}_j$ are the basic matrices coupling the conduction- and valence-band states. They transform according to the irreducible representations contained in the product $X_1 \times X_4$ of the conduction- and valence-band representations. We demonstrate this method in the case of the lowest symmetry under study, C_{2v}.

The four nonequivalent irreducible representations of the C_{2v} point group are shown in Table I together with relevant examples of basic functions. In the C_{2v} point group, the product $X_1 \times X_4$ equals the sum $2B^+ + 2B^-$. This readily allows one to find the basic matrices $\hat{M}_j$ in the bases S,Z and X',Y' defined as $X' = (X - Y)/\sqrt{2}$ and $Y' = (X + Y)/\sqrt{2}$ as follows:

$$\hat{M}_1=\begin{bmatrix}1 & 0\\ 0 & 0\end{bmatrix},\quad \hat{M}_2=\begin{bmatrix}0 & 0\\ 1 & 0\end{bmatrix},$$

$$\hat{M}_3=\begin{bmatrix}0 & 1\\ 0 & 0\end{bmatrix},\quad \hat{M}_4=\begin{bmatrix}0 & 0\\ 0 & 1\end{bmatrix}.$$

As indicated in Table I, the matrix $\hat{M}_1$ or $\hat{M}_2$ transforms according to the representation B^- while $\hat{M}_3$ or $\hat{M}_4$ is the basis matrix of the representation B^+.

As a result, each of the two matrices in Eq. (5) is determined by four linearly independent parameters. In the bases S,Z and X,Y, they have the form

$$V_{\boldsymbol{kp}}=\begin{pmatrix}P_1k_x+P_2k_y & P_1k_y+P_2k_x\\ P_3k_y+P_4k_x & P_3k_x+P_4k_y\end{pmatrix}, \tag{6}$$

$$V_{\mathrm{SO}}=\begin{pmatrix}U_1\sigma_x-U_2\sigma_y & -U_1\sigma_y+U_2\sigma_x\\ -U_3\sigma_y+U_4\sigma_x & U_3\sigma_x-U_4\sigma_y\end{pmatrix}. \tag{7}$$

Here the parameters P_n and U_n $(n=1\div 4)$ are purely imaginary. We note that P_n and U_n describe the properties of interfaces in contrast to the bulk constants $\mathcal{P}$ and $\mathcal{U}$ in Eq. (4). In the envelope-function approach the z dependence of this interface contribution reduces to a δ function as shown in Eq. (5).

By using Eqs. (1) and (5)–(7), one can show that, for a single interface of the C_{2v} symmetry, the correction to the conduction-band Hamiltonian linear in $k_{x,y}$ and responsible for the removal of spin degeneracy is given by

$$\Delta\mathcal{H}_{C_{2\mathrm{v}}}=\begin{pmatrix}1 & 0\\ 0 & 1\end{pmatrix}H_{\mathrm{if}}\delta(z-z_{\mathrm{if}}). \tag{8}$$

Here H_{if} is a linear combination of the spin Pauli matrices that, in the first-order approximation in the perturbations (5), has the form

$$H_{\mathrm{if}}=\frac{\mathcal{P}}{E_0}[(U_3-U_1)h_D(\boldsymbol{k})+(U_4-U_2)h_R(\boldsymbol{k})]$$
$$-\frac{\mathcal{U}}{E_0}[(P_1+P_3)h_D(\boldsymbol{k})+(P_2+P_4)\ h_R(\boldsymbol{k})], \tag{9}$$

with E_0 being the band gap between X_1 and X_4 states.

The electron effective Hamiltonian in an ideal QW contains a sum of two contributions (8) related to the left- (l) and right-hand-side (r) interfaces. If the QW contains an even number of monoatomic layers ($D_{2\mathrm{h}}$ symmetry), then the corresponding parameters U_n^l,U_n^r or P_n^l,P_n^r are interconnected due to S_4 and inversion operations by

$$[U_1,U_2,U_3,U_4]_r=[U_3,U_4,U_1,U_2]_l,$$

$$[P_1,P_2,P_3,P_4]_r=[-P_3,-P_4,-P_1,-P_2]_l.$$

If the QW contains an odd number of monoatomic layers ($D_{2\mathrm{d}}$ symmetry), then

$$[U_1,U_2,U_3,U_4]_r=[U_1,-U_2,U_3,-U_4]_l,$$

$$[P_1,P_2,P_3,P_4]_r=[P_1,-P_2,P_3,-P_4]_l.$$

From here it readily follows that, in the former case, the electronic states in SiGe QWs are spin degenerate ($H_{\mathrm{if}}=0$) and, in the latter, the spin degeneracy is removed by a Dresselhaus-like linear-in-$\boldsymbol{k}$ terms. The similar analysis can be carried out for nonideal SiGe QW structures of the $C_{2\mathrm{v}}$ and $C_{4\mathrm{v}}$ symmetry.

B. Spin splitting of L electrons

Without spin, the basis functions for the L point may be chosen as s like for the L_1 conduction-band state (the Bloch function S'), and as p like (X',Y') for the $L_{3'}$ valence-band states. With spin, they are multiplied by the spin functions $\uparrow$ and $\downarrow$.

In a bulk diamond-lattice semiconductor, the spin-orbit interaction results in a splitting by some value Δ of the $L_{3'}$ valence band into the (L_4^-,L_5^-) and L_6^- subbands. In the three-fold degenerate Γ-point, the second-order perturbation theory with allowance for $\Delta\neq 0$ gives rise to Dresselhaus-like conduction-band spin-splitting in III-V QWs.[8] However, this is not the case for the L point due to large energy spacing between the top valence band $L_{3'}$ (X',Y') and lower-lying valence-band states. Therefore, one should again take into account the interband spin-orbit interaction.

In the bulk, the spin-orbit coupling between the L_1 and $L_{3'}$ bands is forbidden. However, the group C_{s} has only two symmetry operations: the identity and reflection in the (y',z') plane. The reflection yields $\langle S'|U_{x'}|X'\rangle=\langle S'|U_{y',z'}|Y'\rangle=0$, but the following matrix elements are nonzero:

$$U_1'=\langle S'|U_{y'}|X'\rangle,$$

$$U_2'=\langle S'|U_{z'}|X'\rangle,$$

$$U_3'=\langle S'|U_{x'}|Y'\rangle. \tag{10}$$

Introducing the matrix element of the bulk $\boldsymbol{k}\cdot\boldsymbol{p}$-interaction $\mathcal{P}'=(\hbar/m_0)\langle S'|\hat{p}_{x'}|X'\rangle$, we obtain from Eqs. (1) and (10) for the L states in a (001) QW

$$\Delta\mathcal{H}_{C_{\mathrm{s}}}=-\frac{2\mathcal{P}'}{E_0'}\delta(z-z_{\mathrm{if}})(U_2'\sigma_{z'}k_{x'}+U_1'\sigma_{y'}k_{x'}$$
$$+U_3'\sigma_{x'}\langle k_{y'}\rangle). \tag{11}$$

Here E_0' is the energy gap between the L_1 and the $L_{3'}$ states, and the angular brackets mean averaging over the quantum-confined state. As a result the component $k_{y'}=(k_x+k_y-2k_z)/\sqrt{6}$ reduces to $\langle k_{y'}\rangle=(k_x+k_y)/\sqrt{6}$ whereas the component $k_{x'}=(k_x-k_y)/\sqrt{2}$ remains unchanged.

Inclusion of the spin splitting Δ of the valence band slightly modifies the coefficients in the above expression:

$$\Delta\mathcal{H}_{C_s} = -\delta(z-z_{\rm if})\mathcal{P}'\left[\left(\frac{1}{E_0'-\Delta/2}+\frac{1}{E_0'+\Delta/2}\right)U_2'\sigma_{z'}k_{x'}\right.$$
$$+\left(\frac{U_1'+U_3'}{E_0'-\Delta/2}+\frac{U_3'-U_1'}{E_0'+\Delta/2}\right)\sigma_{x'}\langle k_{y'}\rangle$$
$$\left.+\left(\frac{U_1'+U_3'}{E_0'-\Delta/2}+\frac{U_1'-U_3'}{E_0'+\Delta/2}\right)\sigma_{y'}k_{x'}\right].$$

C. Spin splitting in (111)-grown QWs

In (111)-grown QWs the relevant symmetry is C_{3v} with the axis C_3 and two more mirror reflection planes in addition to the elements of C_s group. The rotation yields

$$U_1' = -U_3', \quad U_2' = 0,$$

and we get from Eq. (11) the Rashba-like contribution for the (111) SiGe QWs with odd number of monolayers:

$$\Delta\mathcal{H}_{C_{3V}} = \delta(z'-z_{\rm if})\frac{2\mathcal{P}'U_1'}{E_0'}\ (\sigma_{x'}k_{y'}-\sigma_{y'}k_{x'}). \quad (12)$$

If the number of monolayers is even (D_{3d} symmetry) then the inversion imposes the condition $U_1'=0$, and spin splitting is absent.

IV. DISCUSSION

Within the envelope-function approximation, the electron wave function ψ satisfies the Schrödinger equation with the effective Hamiltonian

$$\mathcal{H} = \mathcal{H}_0(k_z, \boldsymbol{k}) + V(z) + \Delta\mathcal{H}.$$

Here $\mathcal{H}_0$ is the bulk spin-independent Hamiltonian with $k_z = -i\partial/\partial z$, $V(z)$ is the heteropotential, and the correction $\Delta\mathcal{H}$ is given by Eq. (8).

Instead of solving the Schrödinger equation with the Hamiltonian $\mathcal{H}$, one can equivalently find general solutions of the equations $(\mathcal{H}_0+V)\psi = E\psi$ within each homogeneous layer and then apply the boundary conditions

$$\psi(z_{\rm if}-0) = \psi(z_{\rm if}+0),$$

$$(v_z\psi)|_{z_{\rm if}-0} = (v_z\psi)|_{z_{\rm if}+0} + \frac{2i}{\hbar}H_{\rm if}\psi(z_{\rm if}), \quad (13)$$

where the velocity operator $v_z = \hbar^{-1}\partial\mathcal{H}_0/\partial k_z$.

In order to estimate the spin splitting one needs to go beyond the envelope-function approximation. This can be done in the pseudopotential or tight-binding model which yields the matrix $H_{\rm if}$ in boundary conditions (13). The work on estimation of the interface-induced spin splitting in the microscopic tight-binding model is in progress. Here it suffices to note that the spin matrix $H_{\rm if}$ in Eq. (9) is nonvanishing if interatomic contributions to either $H_{\rm SO}$ or $H_{\boldsymbol{kp}}$ are taken into account.

In this paper, we have analyzed spin splitting of electron states in SiGe heterostructures of all possible symmetries. The absence of inversion center can be also probed by means of second-harmonic generation experiments.[5,9,10] An ideal Si_mGe_n superlattice with odd n and m allows second-harmonic generation. It was demonstrated experimentally that Si_mGe_n superlattices with nominally odd and even n, m possess comparable second-harmonic conversion efficiency.[9] The weak nonlinear response can be explained by antiphase microscopic domains shifted with respect to each other by one monoatomic layer along the growth direction [001], see the profiles labeled as D_{4h} in Fig. 1.

Similarly, different domains are characterized by opposite signs of the linear-in-$\boldsymbol{k}$ spin-dependent matrix $H_{\rm if}$ in Eq. (8). The influence of this kind of imperfection on the D'yakonov-Perel' spin relaxation of the conduction electrons depends on the relation between the linear dimension l_D of a single domain and the electron mean free path l in the interface plane. In the case $l_D \gg l$, the spin-relaxation time of free carriers is the same as in a perfect structure:

$$\frac{1}{\tau_s} = \frac{2}{\hbar^2}\langle\tau_p {\rm Tr}(H_{\rm if}^2)\rangle[\psi^\dagger(z_{\rm if})\psi(z_{\rm if})]^2. \quad (14)$$

Here τ_s is the relaxation time of spin z component (for in-plane spin the corresponding time is $2\tau_s$). In Eq. (14) τ_p is the momentum scattering time, the angular brackets mean averaging over the carrier energy distribution, and $\psi(z_{\rm if})$ is the interface value of the envelope function calculated at $H_{\rm if}=0$. In the opposite limiting case $l_D \ll l$, one has

$$\frac{1}{\tau_s(l_D)} \approx \frac{1}{\tau_s}\frac{l_D}{l}, \quad (15)$$

where τ_s is given by Eq. (14). If the time τ_p is governed by scattering from the antiphase-domain walls (boundaries) one can use Eq. (14) for estimations of the spin-relaxation times. Thus, we conclude that, even if the overall symmetry of a SiGe heterostructure is D_{4h} due to the antiphase domains, the lack of inversion center within a particular domain leads to the spin dephasing according to Eqs. (14) and (15).

The presence of domain structure with a shift of both interfaces by one monolayer limits the spin-relaxation time. This upper bound for τ_s has no impurity nature and, hence, does not require random asymmetric doping assumed in Refs. 4 and 11. Our work shows that interfaces produce spin-orbit splitting even in undoped symmetrical SiGe QWs. This opens a possibility to discuss the recent spin-relaxation times measurements in these heterostructures.[2,3]

In conclusion, we have shown that linear-in-$\boldsymbol{k}$ spin splitting is present even in symmetrical SiGe QWs. It can be of Rashba, Dresselhaus, or both types. The splitting is caused by anisotropy of chemical bonds at interfaces.

ACKNOWLEDGMENTS

This work is financially supported by the RFBR, INTAS, "Dynasty" Foundation—ICFPM, and by the Programmes of Russian Ministries of Science and Education.

*Electronic address: golub@coherent.ioffe.ru

[1] S.D. Ganichev, U. Rössler, W. Prettl, E.L. Ivchenko, V.V. Bel'kov, R. Neumann, K. Brunner, and G. Abstreiter, Phys. Rev. B **66**, 075328 (2002).
[2] Z. Wilamowski, W. Jantsch, H. Malissa, and U. Rössler, Phys. Rev. B **66**, 195315 (2002).
[3] Z. Wilamowski and W. Jantsch, Phys. Rev. B **69**, 035328 (2004).
[4] E.Ya. Sherman, Phys. Rev. B **67**, 161303 (2003).
[5] X. Xiao, C. Zhang, A.B. Fedotov, Z. Chen, and M.M.T. Loy, J. Vac. Sci. Technol. B **15**, 1112 (1997).
[6] V.Ya. Aleshkin and N.A. Bekin, J. Phys.: Condens. Matter **9**, 4841 (1997).
[7] Peter Y. Yu and Manuel Cardona, *Fundamentals of Semiconductors. Physics and Material Properties* (Springer-Verlag, Berlin, Heidelberg, 1996).
[8] U. Rössler and J. Kainz, Solid State Commun. **121**, 313 (2002).
[9] D.J. Bottomley, J.-M. Baribeau, and H.M. van Driel, Phys. Rev. B **50**, 8564 (1994).
[10] G. Erley, R. Butz, and W. Daum, Phys. Rev. B **59**, 2915 (1999).
[11] E.Ya. Sherman, Appl. Phys. Lett. **82**, 209 (2003).